

Research Report: Regular Manuscript

Signal diversification is associated with corollary discharge evolution in weakly electric fish

<https://doi.org/10.1523/JNEUROSCI.0875-20.2020>

Cite as: J. Neurosci 2020; 10.1523/JNEUROSCI.0875-20.2020

Received: 15 April 2020

Revised: 11 June 2020

Accepted: 6 July 2020

This Early Release article has been peer-reviewed and accepted, but has not been through the composition and copyediting processes. The final version may differ slightly in style or formatting and will contain links to any extended data.

Alerts: Sign up at www.jneurosci.org/alerts to receive customized email alerts when the fully formatted version of this article is published.

Title: Signal diversification is associated with corollary discharge evolution in weakly electric fish

Abbreviated Title: Corollary discharge evolution in electric fish

Authors: Matasaburo Fukutomi, Bruce A. Carlson

Author Affiliation: Department of Biology, Washington University in St. Louis, St. Louis, Missouri 63130-4899

Corresponding Author: Bruce A. Carlson, E-mail: carlson.bruce@wustl.edu

Number of Pages: 42

Number of Figures: 8

Number of Words

Abstract: 250

Introduction: 647

Discussion: 1824

Conflict of Interest Statement: None

Acknowledgement: This work was supported by the National Science Foundation (Grant IOS-1755071 to B.A.C.) and the Uehara Memorial Foundation (to M.F.). We thank Carl D. Hopkins and Natalie Trzcinski for kindly providing their Knollenorgan recording data; Adalee Lube for assistance with electrophysiology; and Erika Schumacher for assistance with statistical analysis.

Author Contributions: M.F. and B.A.C. designed research; M.F. performed research; M.F. analyzed data; M.F. and B.A.C. wrote the paper.

1 **ABSTRACT**

2 Communication signal diversification is a driving force in the evolution of sensory and motor
3 systems. However, little is known about the evolution of sensorimotor integration. Mormyrid
4 fishes generate stereotyped electric pulses (electric organ discharge [EOD]) for communication
5 and active sensing. The EOD has diversified extensively, especially in duration, which varies
6 across species from 0.1 to over 10 ms. In the electrosensory hindbrain, a corollary discharge that
7 signals the timing of EOD production provides brief, precisely timed inhibition that effectively
8 blocks responses to self-generated EODs. However, corollary discharge inhibition has only been
9 studied in a few species, all with short duration EODs. Here, we asked how corollary discharge
10 inhibition has coevolved with the diversification of EOD duration. We addressed this question by
11 comparing 7 mormyrid species (both sexes) having varied EOD duration. For each individual
12 fish, we measured EOD duration and then measured corollary discharge inhibition by recording
13 evoked potentials from midbrain electrosensory nuclei. We found that delays in corollary
14 discharge inhibition onset were strongly correlated with EOD duration as well as delay to the
15 first peak of the EOD. In addition, we showed that electrosensory receptors respond to self-
16 generated EODs with spikes occurring in a narrow time window immediately following the first
17 peak of the EOD. Direct comparison of time courses between the EOD and corollary discharge
18 inhibition revealed that the inhibition overlaps the first peak of the EOD. Our results suggest that
19 internal delays have shifted the timing of corollary discharge inhibition to optimally block
20 responses to self-generated signals.

21

22 **SIGNIFICANCE STATEMENT**

23 Corollary discharges are internal copies of motor commands that are essential for brain function.
24 For example, corollary discharge allows an animal to distinguish self-generated from external
25 stimuli. Despite widespread diversity in behavior and its motor control, we know little about the
26 evolution of corollary discharges. Mormyrid fishes generate stereotyped electric pulses used for
27 communication and active sensing. In the electrosensory pathway that processes communication
28 signals, a corollary discharge inhibits sensory responses to self-generated signals. We found that
29 fish with long duration pulses have delayed corollary discharge inhibition, and that this time-
30 shifted corollary discharge optimally blocks electrosensory responses to the fish's own signal.
31 Our study provides the first evidence for evolutionary change in sensorimotor integration related
32 to diversification of communication signals.

33

34 **INTRODUCTION**

35 Diversification of communication signals is a driving force in animal speciation. Signal
36 evolution has been associated with evolutionary changes to sensory receptors and central sensory
37 circuits (Osorio and Vorobyev, 2008; Carlson et al., 2011; Baker et al., 2015; ter Hofstede et al.,
38 2015; Vélez and Carlson, 2016; Silva and Antunes, 2016; Vélez et al., 2017; Seeholzer et al.,
39 2018), as well as peripheral effectors and central motor circuits (Bass, 1986; Otte, 1992; Podos,
40 2001; Paul et al., 2015; Ding et al., 2019; Jacob and Hedwig, 2019; Kwong-Brown et al., 2019).
41 Despite this accumulated knowledge of sensory and motor system evolution, we know little
42 about the evolution of sensorimotor interactions between these systems.

43 Corollary discharges are one of the links by which motor control influences sensory
44 processing to distinguish external from self-generated stimuli (von Holst and Mittelstaedt, 1950;
45 Sperry, 1950; Poulet and Hedwig, 2007; Crapse and Sommer, 2008; Schneider and Mooney,
46 2018; Straka et al., 2018). For communicating animals, a corollary discharge generally works to
47 filter out an animal's own signals (reafference), allowing selective sensory processing of signals
48 from other individuals (exafference). Since a corollary discharge needs to selectively cancel
49 reafferent input, its function should evolve to adapt to signal diversification. However, this
50 question has not been addressed to our knowledge.

51 Here we investigate corollary discharge evolution in mormyrids, African weakly electric
52 fishes. These fish produce electric-pulse signals, termed electric organ discharge (EOD), that are
53 used for electrolocation and communication (Hopkins, 1999; von der Emde, 1999). EOD
54 waveforms are stereotyped but diverse among species and sometimes among individuals within
55 species (Hopkins, 1981; Arnegard et al., 2010; Paul et al., 2015; Gallant and O'Connell, 2020).
56 The EOD is generated from an electric organ (EO) at the base of the tail (Fig. 1A; Bennett, 1971).

57 EOD waveform is determined by the biophysical characteristics of electrocytes in the EO, while
58 EOD timing is determined by central neural commands (Bennett, 1971; Bass, 1986; Carlson,
59 2002a).

60 Electric communication signals are processed by a dedicated sensory pathway (Fig. 1A;
61 Xu-Friedman and Hopkins, 1999; Baker et al., 2013). Sensory receptors called Knollenorgans
62 (KO) respond to outside-positive changes in voltage across the skin, or inward current, with a
63 fixed latency spike (Bell, 1989). Because each KO faces out towards the surrounding water, in
64 response to an external EOD, KOs on one side of the body receive an inward current while KOs
65 on the other side receive an outward current (Hopkins and Bass, 1981). By contrast, in response
66 to a self-generated EOD, KOs on both sides receive the same-direction currents of the waveform
67 consisting of a large outward current followed by a large inward current if the EOD has a head-
68 positive polarity (Fig. 1A). The KO afferent fibers project to the nucleus of the electrosensory
69 lateral line lobe (nELL) in the hindbrain, where corollary discharge inhibition blocks responses
70 to the fish's own EOD (Fig. 1A; Bell and Grant, 1989). The axons of nELL neurons project to
71 the anterior extero-lateral nucleus (ELa) of the midbrain torus semicircularis, which sends its only
72 output to the posterior extero-lateral nucleus (ELp) (Fig. 1A; Xu-Friedman and Hopkins, 1999).

73 Mormyrids are advantageous for studying corollary discharge interactions between motor
74 and sensory systems: the motor command signal (fictive EOD) can be easily recorded from
75 spinal electromotor neurons (EMN) when EOD production is silenced pharmacologically.
76 Previous studies reported that corollary discharge inhibition starts about 2 ms after the onset of
77 command signal and lasts for about 2 ms (Fig. 1B; Amagai, 1998; Lyons-Warren et al., 2013b;
78 Vélez and Carlson, 2016). Those studies used limited species that have short-duration EODs
79 (~0.5 ms), but the mormyrid family has evolved EOD durations ranging from 0.1 to over 10 ms

80 (Hopkins, 1999). The present study uses 7 mormyrid species having EODs that vary in duration
81 from ~0.1 to ~10 ms, and compares corollary discharge inhibition across species to reveal
82 evolutionary change of corollary discharge in relation to signal diversification.
83

84 **MATERIALS AND METHODS**

85 All procedures were in accordance with guidelines established by the National Institutes of
86 Health and were approved by the Animal Care and Use Committee at Washington University in
87 St Louis.

88

89 *Animals*

90 6 *Brienomyrus brachyistius* (Standard length [SL] = 7.5–11.8 cm), 3 *Brevimyrus niger* (SL =
91 6.7–9.5 cm), 3 *Campylomormyrus compressirostris* (SL = 11.8–14.0 cm), 6 *Campylomormyrus*
92 *numenius* (SL = 12.4–14.2 cm), 4 *Campylomormyrus tamandua* (SL = 6.5–9.1 cm), 3
93 *Gnathonemus petersii* (SL = 10.2–11.6 cm) and 2 *Mormyrus tapirus* (SL = 12.3–12.3 cm)
94 contributed EOD and evoked potential data to this study. We used fish of both sexes in *B.*
95 *brachyistius*, *B. niger*, *C. numenius* and *C. tamandua*, but only female in *C. compressirostris*, *G.*
96 *petersii* and *M. tapirus*. Subsets of these fish (1 *B. brachyistius*, 1 *C. compressirostris* and 1 *C.*
97 *numenius*) were used for simultaneous recording of the EOD and EOD command generated by
98 EMNs. All fish were purchased from Bailey Wholesale Tropical Fish (San Diego, CA) and
99 AliKhan Tropical Fish LLC (Richmond Hill, NY). The fish were housed in water with a
100 conductivity of 175–225 $\mu\text{S}/\text{cm}$, a pH of 6–7, and a temperature of 25–29 °C. The fish were kept
101 on a 12/12-h light/dark cycle and fed live black worms 4 times a week.

102

103 *EOD recording and analysis*

104 We recorded 10 EODs from each fish while it was freely swimming. EODs were amplified 10
105 times, band-pass filtered (1 Hz–50 kHz) (BMA-200, Ardmore), digitized at a rate of 195 kHz
106 (RP2.1, Tucker Davis Technologies), and saved using custom software in Matlab (Mathworks).

107 EODs generally consist of peak 1 (maximum head-positive peak) and peak 2 (maximum
108 head-negative peak). Some species we recorded from (*B. brachyistius*, *B. niger*, *C. tamandua*
109 and *G. petersii*) have EODs with an additional peak 0 (small head negative peak before peak 1).
110 For EODs without a peak 0, EOD onset was determined as the point crossing 2% of peak-1
111 amplitude. For EODs with a peak 0, EOD onset was determined as the point crossing 20% of
112 peak-0 amplitude. In both cases, EOD offset was determined as the point crossing 2% of peak-2
113 amplitude. EOD duration was determined as the period between EOD onset and offset. Delay to
114 peak 1 was determined as the period between EOD onset and timing of peak 1. In addition, EOD
115 frequency content was calculated by fast Fourier transformation.

116 We grouped EODs of *C. numenius* into three arbitrary types based on variation in
117 duration (Long, Intermediate, and Short EOD), following a previous study that revealed
118 extensive individual variation in EOD duration within this species (Paul et al., 2015). In the
119 following analysis, we used the average value without separating types.

120

121 *Simultaneous recording and analysis of EOD and EOD command*

122 This recording session was performed after EOD recording and before evoked potential
123 recording only for three fish. Fish were anesthetized in a solution of 300 mg/L tricaine
124 methanesulfonate (MS-222) (Sigma-Aldrich) and positioned on a plastic platform in a recording
125 chamber filled with fresh water. Fish were restrained by lateral plastic pins and a plastic tube on
126 the tail. Freshwater was provided through a pipette tip in the fish's mouth. EOD commands from
127 spinal EMNs were recorded with a pair of electrodes located within the plastic tube and oriented
128 parallel to the fish's EOD, amplified 1,000 times, and band-pass filtered (10 Hz–5 kHz) (Model
129 1700, A-M systems). While EOD commands from EMNs were recorded, the EODs were

130 recorded by separate electrodes, amplified 10 times and band-pass filtered (1 Hz–50 kHz)
131 (BMA-200, Ardmore). These recordings were digitized at a rate of 1 MHz and saved (TDS
132 3014C, Tektronix). We recorded 9–11 trials from each fish.

133 EOD command traces from EMNs were averaged across trials, and EOD traces were
134 filtered by a 21st-order median filter whose time window was 0.02 ms and averaged across trials.
135 EOD onset was determined in the same way we determined EOD onset in freely swimming EOD
136 recordings. Delay to EOD onset (D_{Onset}) was calculated as the period between EOD command
137 onset and EOD onset. Delay to peak 1 of EOD (D_{P1}) from EOD command was calculated as the
138 sum of D_{Onset} and the delay between EOD onset and peak 1 recorded from freely swimming fish.

139

140 *Surgery and evoked potential recording*

141 This recording session was performed after EOD recording (or simultaneous recording of EODs
142 and EOD commands for the three fish). We prepared fish for *in vivo* recordings from ELa and
143 ELp as described previously (Carlson, 2009, Lyons-Warren et al., 2013a). Briefly, fish were
144 anesthetized in 300 mg/L MS-222 and paralyzed with an intramuscular injection of 0.1 mL of
145 3.0 mg/mL gallamine triethiodide (Flaxedil) (Sigma-Aldrich). The fish were then transferred to a
146 recording chamber (20 × 12.5 × 45 cm) filled with water and positioned on a plastic platform,
147 leaving a small region of the head above water level. During surgery, we maintained general
148 anesthesia by respirating the fish with an aerated solution of 100 mg/mL MS-222 through a
149 pipette tip placed in the mouth. For *Campylomormyrus* species, we connected a hose made from
150 heat shrink tubing to the pipette tip so as to provide respiration to the long, tube-like mouth. For
151 local anesthesia, we applied 0.4% Lidocaine on the skin overlying the incision site, and then
152 made an incision to uncover the skull overlying the ELa and ELp. Next, we glued a head post to

153 the skull before using a dental drill and forceps to remove a rectangular piece of skull covering
154 the ELa and ELp. In *Campylomormyrus* species, the ELa and ELp are not exposed superficially,
155 so we exposed ELa and ELp by separating the optic tectum and the valvula cerebellum using two
156 retractors made from borosilicate capillary glass (Vélez and Carlson, 2016; Vélez et al., 2017).
157 After exposing ELa and ELp, we placed a reference electrode on the nearby cerebellum.
158 Following surgery, we switched respiration to fresh water and allowed the fish to recover from
159 general anesthesia. We monitored the anesthetized state of the fish with a pair of electrodes
160 oriented parallel to its EO within a plastic tube to record fictive EOD commands produced by the
161 EMNs (Carlson, 2009; Lyons-Warren et al., 2013a). These EOD commands were 1,000x
162 amplified (Model 1700, A-M systems) and sent to a window discriminator for time stamping
163 (SYS-121, World Precision Instruments). At the end of the recording session, the respiration of
164 the fish was switched back to 100 mg/L MS-222 until no fictive EOD could be recorded, and
165 then the fish was sacrificed by freezing.

166 Evoked potentials in ELa and ELp were obtained with glass microelectrodes made of
167 borosilicate capillary glass (o.d. = 1.0 mm, i.d. = 0.5 mm; Model 626000, A-M Systems) pulled
168 on a micropipette puller (Model P-97, Sutter Instrument Company), broken to a tip diameter of
169 10–20 μm and filled with 3M NaCl solution. Evoked potentials were 1,000x amplified, band-
170 pass filtered (10 Hz–5 kHz) (Model 1700, A-M systems), digitized at a rate of 97.7 kHz (RX 8,
171 Tucker Davis Technologies) and saved using custom software in Matlab (Mathworks).

172

173 *Sensory stimulation*

174 We used three vertical electrodes on each side of the recording chamber (anodal to the fish's left,
175 cathodal to the right) to deliver transverse stimuli with normal polarity (peak preceding trough).

176 Digital stimuli were generated using custom software in Matlab, converted to analog signals with
177 a signal processor (RX8, Tucker Davis Technologies), attenuated with an attenuator (PA5,
178 Tucker Davis Technologies) and isolated from ground with a stimulus isolation unit (Model
179 2200, A-M Systems).

180 To examine corollary discharge inhibition of sensory responses, we delivered 0.2 ms
181 bipolar square pulses at several delays following the EOD command onset. Because KOs
182 respond with time-locked spikes to the edges of square pulses (Bennett, 1965; Hopkins and Bass,
183 1981; Lyons-Warren et al., 2012; Baker et al., 2015), this short square-pulse stimulation allowed
184 us to precisely control the timing of sensory input to the KO system and quantify the timing of
185 corollary discharge inhibition in nELL. The EOD command onset was determined as the first
186 negative peak of the EOD command waveform that consists of a three-spike potential resulting
187 from the synchronous activation of EMNs. Each delay was repeated 10 times and the averaged
188 response was used for analysis. First, we recorded sensory responses in the ELp at delays
189 between 0 and 20 ms in 0.5-ms steps. Based on these initial data, we used custom software
190 written in R to determine the range of delays to examine corollary discharge inhibition with
191 higher time resolution. The algorithm included the following steps: (1) calculated peak-to-peak
192 amplitudes as a measure of response across all delays, (2) normalized all responses to the
193 maximum response, (3) determined the latency resulting in the minimum response amplitude, (4)
194 determined the onset and offset delays that resulted in responses just less than 80% of the
195 maximum response, (5) determined the range of delays to examine corollary discharge inhibition
196 with higher time resolution as 2 ms before the onset time to 2 ms after the offset time. Then, we
197 recorded sensory responses in the ELp to stimulus delays across this range in 51 equally spaced
198 steps (~ 0.1–0.2 ms). After recording in the ELp, we recorded sensory responses in the ELa using

199 the same stimulus delays used in both the broad and narrow ranges tested in ELP. The stimulus
200 sequences were randomized in all recordings.

201 To observe clear corollary discharge inhibition, we needed to decide on an adequate
202 stimulus intensity for each tested individual before measuring of corollary discharge. First, we
203 recorded evoked potentials at 0, 3, 4 and 5 ms delays at 20 dB attenuation (reference intensity of
204 736 mV/cm) and determined peak-to-peak amplitudes of each delay. Then, we calculated ratios
205 of peak-to-peak amplitudes at 3, 4 and 5 ms delay to one at 0 ms delay. If the minimum ratio was
206 under 30%, we chose this stimulus intensity. If the ratio was above 30%, we reduced the
207 intensity by adding 5 dB attenuation and performed above recording until the ratio got under
208 30%. From this procedure, we chose 23.4 mV/cm for 1 *C. compressirostris* and 73.6 mV/cm for
209 all the other fishes.

210

211 *Evoked potential recording analysis*

212 We characterized corollary discharge inhibition with respect to timing and duration. All analyses
213 here were done using the recordings from the high resolution, narrow range of stimulus delays.
214 Normalized amplitude was calculated by the following steps: (1) calculated peak-to-peak
215 amplitude for each delay, (2) subtracted by the minimum peak-to-peak amplitude across all
216 delays and (3) divided by the maximum peak-to-peak amplitude across all delays, which leads to
217 setting the maximum value as 1 and the minimum value as 0. Then, we set an 80% threshold to
218 determine the inhibition onset, offset, and duration. In addition, we determined the peak time of
219 inhibition as the stimulus delay at which the response amplitude was minimal.

220

221 *KO recording and analysis*

222 KO recording data from *B. brachyistius* (n = 6 KOs), *B. niger* (n = 5), *Campylomormyrus alces*
223 (n = 1), *C. compressirostris* (n = 7), *C. numenius* (n = 2) and *C. tamandua* (n = 2) came from
224 previously published studies (Trzcinski, 2008; Trzcinski and Hopkins, 2008; Lyons-Warren et al.,
225 2012; Baker et al., 2015). Based on a recent study of *Campylomormyrus* species (Paul et al.,
226 2015), we concluded that *Campylomormyrus sp.* B shown in Trzcinski (2008) and Trzcinski and
227 Hopkins (2008) was *C. numenius*.

228 The recording methods were generally shared among these previous studies. Similar to
229 our evoked potential recording, fish were immobilized with Flaxedil, transferred to a recording
230 chamber filled with freshwater and positioned on a plastic platform with lateral support. The fish
231 were provided freshwater through a pipette tip in the fish's mouth while monitoring the fish's
232 EOD command signals using a pair of electrodes placed next to the fish's tail. Extracellular
233 recordings of KO spikes were made using a wire electrode inside glass capillary tubing that was
234 placed directly next to a KO. The signals were amplified, digitized, and recorded with custom
235 software in Matlab. Sensory stimuli consisted of conspecific EOD waveforms generated in
236 Matlab, digital-to-analog converted, attenuated, and delivered as a constant-current stimulus
237 through the electrode.

238 These previous studies recorded KO responses to multiple waveforms at several
239 intensities. For each recording, relative but not absolute intensities were known, because the
240 amount of current going into the electroreceptor pore is dependent upon the position of the
241 electrode tip relative to the pore, the size and shape of the pore, and the resistive paths between
242 the electrode tip and the pore. Importantly, however, self-generated EODs will be of relatively
243 large intensity. We therefore chose among these data here using the following criteria: (1) the
244 EOD waveform stimulus was the inverted form of a conspecific EOD recorded with recording

245 electrode at the head and reference electrode at the tail to simulate the self-generated EOD
246 waveform; and (2) the largest stimulus intensity tested that did not result in a stimulus artifact
247 that exceeded KO spike amplitude.

248 To calculate normalized KO responses, we made peristimulus time histograms (bin size =
249 0.02048 ms) of KO spikes and normalized them by the maximum spike counts. Delay to peak
250 KO response was determined as the period between the onset of the EOD stimulus and the time
251 of the maximum KO response.

252

253 *Experimental design and statistical analysis*

254 The primary objective of this study was to determine the relationship between EOD waveform
255 and corollary discharge inhibition. We used 7 species including 27 fishes, and recorded EODs
256 from freely swimming individuals followed by evoked potential recording from the midbrain.
257 Subsequently, we asked whether corollary discharge inhibition overlapped KO spike timing to
258 block responses to self-generated EODs. To compare the time courses between corollary
259 discharge inhibition and EOD using an identical reference of EOD command onset, we
260 performed simultaneous recording of EOD and EOD command from a subset (3 species
261 including 3 fishes) of them before performing electrophysiology. Furthermore, we measured KO
262 response latency to self-generated EODs using previously published data (Trzcinski, 2008;
263 Trzcinski and Hopkins, 2008; Lyons-Warren et al., 2012; Baker et al., 2015).

264 Although corollary discharge inhibition occurs in nELL (Mugnaini and Maler, 1987; Bell
265 and Grant, 1989), we focused on the downstream pathway, ELa and ELp. There are two reasons
266 for this. First, neural recordings from nELL are much more challenging because it is a deep
267 structure whereas ELa and ELp are superficial structures. Second, recordings from nELL reveal

268 complex evoked potentials consisting of sensory responses time-locked to the stimulus as well as
269 corollary discharge inhibition time-locked to the EOD command, and these occur at different
270 relative times for different stimulus delays (Bell and Grant 1989). By contrast, recordings from
271 the downstream target of nELL allow us to isolate sensory evoked potentials from corollary
272 discharge potentials and measure the effects of corollary discharge inhibition in nELL (Russell
273 and Bell, 1978). We recorded from both ELa and ELp, because the present study includes several
274 species (*C. compressirostris*, *C. numenius*, *C. tamandua* and *M. tapirus*) for which evoked
275 potential recordings from ELa and ELp had never before been published. We therefore recorded
276 from both nuclei in all individuals studied to compare among the species, and determine whether
277 the response characteristics of ELa and ELp in unstudied species were similar to previously
278 studied species.

279 Here we recorded evoked field potentials rather than single-unit spiking activities.
280 Individual neurons in ELa and ELp show diversity both in terms of cellular types (afferents,
281 efferents and interneurons) and sensory tuning within the types (Carlson, 2009; Baker et al.,
282 2013; Lyons-Warren et al., 2013b). This would require very large numbers of recordings to
283 accurately capture the corollary discharge effects. Field potential recording is a reliable and
284 relatively simple technique that provides valuable insights into integrative processes within brain
285 nuclei (Einevoll et al., 2013). Although the biophysical basis of local field potentials is disputed,
286 it clearly represents summated electrical activity of neurons, which may reflect neuronal spiking
287 and synaptic activity in the vicinity of the recording electrode. The aim of the present study was
288 not to quantify the strength of inhibition in individual neurons, but the timing and duration of
289 inhibitory effects across the population. Indeed, many previous studies used evoked potential
290 recordings from ELa and ELp and showed clear and reliable corollary discharge inhibition in

291 some mormyrid species (Russell and Bell, 1978; Amagai, 1998; Lyons-Warren et al., 2013b;
292 Vélez and Carlson, 2016). Therefore, evoked field potential recording is ideal for the purposes of
293 the present study.

294 For statistical analysis, we used a phylogenetic generalized least squares (PGLS) model
295 with a Brownian correlation structure to account for phylogenetic effects on the correlation
296 analyses. For cross-species correlation analyses, it is necessary to incorporate phylogenetic
297 information into a model because the lack of independence between data points of varying
298 relatedness violates the assumptions of standard linear regression (Grafen, 1989; Mundry, 2014).
299 We used a previously constructed bootstrapped maximum-likelihood tree from 73 Cytb
300 osteoglossomorph sequences (Sullivan et al., 2000; Lavoué et al., 2003; Feulner et al., 2008;
301 Sukhum et al., 2018). To include data from species that have not been sequenced, we used
302 sequence data from within monophyletic genera and chose the species sequence with the shortest
303 phylogenetic distance from the genus node. In this analysis, we used average values within
304 species of EOD waveform, corollary discharge inhibition, and KO response. Using this PGLS
305 model, we estimated both the slope and the intercept of the regression line and calculated t-
306 values, p-values, and 95% confidence intervals (CI) for each parameter. We used the t-value and
307 p-value to determine whether a given parameter was significantly different from zero. All
308 phylogenetic analyses were performed in R programming software with the ape and nlme
309 packages (Paradis and Schliep, 2018; Pinheiro et al., 2020). To examine individual differences
310 within *C. numenius*, we used standard linear regression analysis rather than PGLS.

311

312 **RESULTS**313 **Mormyrids have diverse species-specific EODs**

314 To relate corollary discharge inhibition to EOD waveform, we recorded EODs individually from
315 7 species before performing evoked potential recordings (Fig. 2A). EOD duration varied widely
316 across species, from as short as 0.17 ms in *C. compressirostris* to as long as 8.59 ms in *C.*
317 *numenius* (Fig. 2B). Fast Fourier transformation revealed that peak power frequencies ranged
318 from 110 Hz in *C. numenius* to 7610 Hz in *C. compressirostris* (Fig. 2C, D).

319

320 **Corollary-discharge timing and duration varies among species**

321 To measure the inhibitory effect of corollary discharge in the KO pathway, we performed evoked
322 potential recordings from ELa and ELp (Fig. 3A). We stimulated with 0.2-ms bipolar square
323 electric pulses delivered with a delay of 0–20 ms following the EOD command from spinal
324 electromotor neurons (EMNs) (Fig. 3A). To our knowledge, these are the first evoked potential
325 recordings from the midbrain of *Campylomormyrus* species and *M. tapirus*. The recording traces
326 of evoked potentials from those species were similar to those of previously reported species,
327 including *B. brachyistius*, *B. niger*, *G. petersii*, *Petrocephalus microphthalmus* and
328 *Petrocephalus tenuicauda* (Russell and Bell, 1978; Amagai, 1998; Carlson, 2009; Lyons-Warren
329 et al., 2013b; Vélez and Carlson, 2016): electrosensory stimulation elicited sharp and short-
330 latency (~2–4 ms) evoked potentials in ELa, and broad and longer-latency (~6–10 ms) evoked
331 potentials in ELp (Fig. 3B). We also tested whether response latencies in ELa to the short square-
332 pulse stimulus was correlated with EOD duration among species, but the response latency was
333 independent of EOD duration (estimated slope = 0.01 ms/ms, 95% CI = -0.08 – 0.10 ms/ms, $t_{(5)}$
334 = 0.37, $p = 0.73$; estimated intercept = 2.9 ms, 95% CI = 2.3 – 3.6 ms, $t_{(5)} = 11.7$, $p = 0.0001$).

335 In each species, we found a narrow range of stimulus delays for which electrosensory
336 responses were blocked by corollary discharge inhibition (Fig. 3C), as shown previously in *B.*
337 *brachyistius* and *B. niger* (Amagai, 1998; Lyons-Warren et al., 2013b; Vélez and Carlson, 2016).
338 From these evoked potential traces, we determined the corollary discharge inhibition window for
339 each individual using normalized amplitudes and an 80% cutoff line (Fig. 3D). This revealed that
340 corollary discharge onset, offset, duration, and peak time varied among species (Fig. 3D). For
341 example, evoked potentials in the short-EOD *C. compressirostris* were blocked when sensory
342 stimuli were delivered with a 3-4 ms delay following the EOD command, whereas evoked
343 potentials in the long-EOD *C. numenius* were blocked when stimuli were delivered with a 5-6 ms
344 delay following the EOD command (Fig. 3C).

345

346 **Corollary discharge timing is correlated with EOD waveform**

347 We next asked whether species diversity in EOD waveform (Fig. 2) was correlated with species
348 diversity in corollary discharge timing (Fig. 3). First, we tested the relationship between EOD
349 duration and corollary discharge inhibition duration (Fig. 4A, B). Inhibition duration in EL_a was
350 positively correlated with EOD duration (Fig. 4A; estimated slope = 0.20 ms/ms, 95% CI = 0.10
351 – 0.29 ms/ms, $t_{(5)} = 5.1$, $p = 0.004$; estimated intercept = 2.4 ms, 95% CI = 1.7 – 3.1 ms, $t_{(5)} =$
352 8.6, $p = 0.0004$), whereas inhibition duration in EL_p was not correlated with EOD duration (Fig.
353 4B; estimated slope = 0.01 ms/ms, 95% CI = -0.29 – 0.30 ms/ms, $t_{(5)} = 0.05$, $p = 0.96$; estimated
354 intercept = 3.3 ms, 95% CI = 1.1 – 5.5 ms, $t_{(5)} = 3.9$, $p = 0.01$).

355 The different timing of corollary discharge inhibition in species with different EOD
356 durations (Fig. 3C, D) suggested that corollary discharge onset rather than duration might be
357 associated with EOD duration. Indeed, we found that inhibition onset was strongly correlated

358 with EOD duration in both ELa (Fig. 4C; estimated slope = 0.27 ms/ms, 95% CI = 0.19 – 0.36
359 ms/ms, $t_{(5)} = 8.0$, $p = 0.0005$; estimated intercept = 2.4 ms, 95% CI = 1.8 – 3.1 ms, $t_{(5)} = 9.5$; $p =$
360 0.0002) and ELp (Fig. 4D; estimated slope = 0.28 ms/ms, 95% CI = 0.21 – 0.35 ms/ms, $t_{(5)} =$
361 10.1, $p = 0.0002$; estimated intercept = 2.3 ms, 95% CI = 1.8 – 2.8 ms, $t_{(5)} = 11.1$, $p = 0.0001$).

362 Here we recall two important features of KO responses to self-generated EODs: (1) each
363 receptor responds with time-locked spikes to outside-positive changes in voltage across the skin;
364 and (2) all KOs receive the same EOD waveform, which is inverted in polarity compared to the
365 head-positive EOD recordings shown in Fig. 2. This suggests that KOs should respond
366 immediately after peak 1 of the EOD, when the self-generated EOD transitions from a negative
367 to positive peak. This further suggests that, in order to effectively block responses to self-
368 generated EODs, the timing of corollary discharge inhibition should also relate to the timing of
369 EOD peak 1. Indeed, we found that inhibition onset was strongly correlated with the delay to
370 EOD peak 1 in both ELa (Fig. 4E; estimated slope = 0.92 ms/ms, 95% CI = 0.60 – 1.24 ms/ms, $t_{(5)}$
371 $= 7.5$, $p = 0.0007$; estimated intercept = 2.3 ms; 95% CI = 1.6 – 3.0 ms, $t_{(5)} = 8.4$, $p = 0.0004$)
372 and ELp (Fig. 4F; estimated slope = 0.94 ms/ms, 95% CI = 0.68 – 1.20 ms/ms, $t_{(5)} = 9.4$, $p =$
373 0.0002; estimated intercept = 2.2 ms, 95% CI = 1.6 – 2.7 ms, $t_{(5)} = 9.8$, $p = 0.0002$). The fact that
374 the slopes were close to 1 indicates a 1:1 correspondence between the corollary discharge delay
375 and delay to EOD peak 1.

376 Since our definition of EOD duration requires arbitrary cutoffs to define the beginning
377 and end of the EOD, we also determined whether EOD peak power frequency correlated with
378 inhibition duration and onset. We found a significant negative correlation between peak power
379 frequency and inhibition duration in ELa (estimated slope = -0.14 ms/kHz, 95% CI = -0.19 – -
380 0.09 ms/kHz, $t_{(5)} = -7.1$, $p = 0.0008$; estimated intercept = 3.1 ms, 95% CI = 2.6 – 3.7 ms, $t_{(5)} =$

381 13.9, $p = 3.4 \times 10^{-5}$), but this relationship was not significant in ELP (estimated slope = -0.04
382 ms/kHz, 95% CI = -0.23 – 0.16 ms/kHz, $t_{(5)} = -0.47$, $p = 0.66$; estimated intercept = 3.5 ms, 95%
383 CI = 1.2 – 5.7 ms, $t_{(5)} = 3.9$, $p = 0.01$). By contrast, there were significant negative correlations
384 between peak power frequency and inhibition onset in both ELA (estimated slope = -0.19 ms/kHz,
385 95% CI = -0.23 – -0.15 ms/kHz, $t_{(5)} = -11.6$, $p = 0.0001$; estimated intercept = 3.4 ms, 95% CI =
386 2.9 – 3.9 ms, $t_{(5)} = 17.9$, $p = 1.0 \times 10^{-5}$) and ELP (estimated slope = -0.19 ms/kHz, 95% CI = -
387 0.23 – -0.16 ms/kHz, $t_{(5)} = -14.8$, $p = 2.5 \times 10^{-5}$; estimated intercept = 3.3 ms, 95% CI = 2.9–3.7
388 ms, $t_{(5)} = 21.8$, $p = 3.8 \times 10^{-6}$).

389

390 **KO responses to self-generated EODs depend on the delay to peak 1**

391 We tested the hypothesis that KO responses are time-locked to peak 1 of the EOD in both short-
392 EOD and long-EOD species. We used previously published data from 6 species (Trzcinski,
393 2008; Trzcinski and Hopkins, 2008; Lyons-Warren et al., 2012; Baker et al., 2015) and examined
394 the timing of KO spiking responses to conspecific EODs. By convention, ‘normal’ EOD polarity
395 is defined as a waveform recorded with the recording electrode at the head and a reference
396 electrode at the tail as shown in Fig. 2. Here we focused on KO responses to ‘inverted’ EODs
397 that represent the same waveform that KOs receive in response to self-generated EODs. We
398 found that KOs responded with time-locked spikes with short delay following peak 1 of the EOD
399 (Fig. 5A; delays between peak 1 of EOD and peak KO response were 0.14 ms in *C.*
400 *compressirostris*, 0.07 ms in *B. brachyistius* and 0.37 ms in *C. numenius*). Across species, delay
401 to peak KO response strongly correlated with delay to peak 1 of the EOD (Fig. 5B; estimated
402 slope = 1.15 ms/ms, 95% CI = 1.07 – 1.23 ms/ms, $t_{(4)} = 40.0$, $p = 2.3 \times 10^{-6}$; estimated intercept
403 = 0.09 ms, 95% CI = -0.10 – 0.28 ms, $t = 1.3$, $p = 0.26$).

404

405 **Corollary discharge inhibition timing blocks KO responses to self-generated EODs**

406 Our results so far revealed that corollary discharge inhibition and KO spiking responses were
407 both correlated with delay to peak 1 of the EOD. This leads to the further question of whether the
408 time-shifted corollary discharge inhibition actually blocks response to self-generated EODs. To
409 address this question, we measured the delay between the EOD command from spinal motor
410 neurons and the EOD in fish that were not electrically silenced and paralyzed. We found that
411 delays between EOD command onset and EOD onset were similar among the three species (*C.*
412 *compressirostris*, 3.12 ms; *B. brachyistius*, 3.08 ms; *C. numenius*, 3.28 ms) (Fig. 6). Thus, the
413 delays between EOD command onset and peak 1 of the EOD varied among the species (*C.*
414 *compressirostris*, 3.24 ms; *B. brachyistius*, 3.41 ms; *C. numenius*, 5.05 ms) (Fig. 6). Comparing
415 the time courses of the EOD and corollary discharge inhibition using an identical reference of the
416 EOD command onset revealed that corollary discharge inhibition overlapped with the timing of
417 EOD peak 1 across species (Fig. 6).

418

419 **Corollary discharge inhibition timing is correlated with individual EOD waveform**
420 **variation within *C. numenius***

421 The high degree of individual variation in EOD duration in *C. numenius* (Fig. 2A, B) facilitates
422 an examination of the correlation between EOD waveform and corollary discharge within
423 species. Similar to our results across species, corollary discharge onset was strongly correlated
424 with delay to peak 1 of the EOD in both ELa (Fig. 7A; estimated slope = 0.43 ms/ms, 95% CI =
425 0.24 – 0.62 ms/ms, $t_{(4)} = 6.4$, $p = 0.003$; estimated intercept = 3.1 ms, 95% CI = 2.8 – 3.4 ms, $t_{(4)} = 27.0$, $p = 1.1 \times 10^{-5}$) and ELp (Fig. 7B; estimated slope = 0.48 ms/ms, 95% CI = 0.25 – 0.70

427 ms/ms, $t_{(4)} = 5.8$, $p = 0.004$; estimated intercept = 2.8 ms, 95% CI 2.4 – 3.2 ms, $t_{(4)} = 20.2$, $p =$

428 3.5×10^{-5}).

429 **DISCUSSION**

430 Our findings provide evidence that diverse communication signals in mormyrids are correlated
431 with corollary discharge inhibition of the electrosensory pathway. We show that EOD duration is
432 only weakly correlated with the duration of corollary discharge inhibition, but strongly correlated
433 with the onset of corollary discharge inhibition (Fig. 4). Taking into account that electroreceptors
434 (KOs) produce spikes with short latency following peak 1 of the EOD (Fig. 5) and that the
435 corollary discharge inhibition overlaps this peak (Fig. 6), we conclude that corollary discharge
436 inhibition has evolved to shift its time window so as to optimally block KO spikes in response to
437 self-generated EODs (Fig. 8).

438 Evolutionary change in behavior can result from changes to sensory systems, motor
439 systems, or both (Katz, 2011, 2016; Martin, 2012; Stöckl and Kelber, 2019). Correlated
440 evolution of sensory and motor systems is especially apparent in communication systems, as this
441 requires evolutionary change in both signal production and reception (Bass and Hopkins, 1984;
442 Bass, 1986; Otte, 1992; ter Hofstede et al., 2015; Silva and Antunes, 2016). Indeed, mormyrids
443 show correlated evolution between senders and receivers of their electric communication signals:
444 the frequency tuning of KOs is related to the frequency spectrum of conspecific EODs (Bass and
445 Hopkins, 1984; Lyons-Warren et al., 2012; but see also Baker et al., 2015). Here we add a
446 further insight that signal evolution accompanies evolutionary change of neural circuitry
447 underlying sensorimotor integration. Corollary discharges that filter sensory responses to self-
448 generated signals are ubiquitous across communicating animals (Crapse and Sommer, 2008). In
449 addition, signals among related species often vary widely in temporal features (Otte, 1992;
450 Hopkins, 1999; Podos, 2001), and changing the timing of communication signals alters the
451 timing of reafferent input. Therefore, we expect similar evolutionary change in corollary

452 discharge timing to be widespread across sensory modalities and taxa. For example, the temporal
453 structures of species-specific songs of crickets are similarly diverse to mormyrid EODs (Otte,
454 1992; ter Hofstede et al., 2015), and a similar corollary discharge inhibition of the auditory
455 pathway has been described in one species (Poulet and Hedwig, 2006).

456 Why does evolutionary change of EOD duration relate to the delay of corollary discharge
457 inhibition rather than inhibition duration? Theoretically, it is possible to alter the duration to
458 cover the entirety of EODs with different durations. However, changing the delay of corollary
459 discharge inhibition without expanding the duration would avoid unnecessarily elongating the
460 resulting insensitive period. This is because the KOs responding to self-generated EODs produce
461 spikes only over a narrow window of time just after EOD peak 1 regardless of EOD duration
462 (Fig. 5). Accordingly, we suggest an optimal evolutionary strategy for modifying corollary
463 discharge inhibition during signal evolution: minimizing the inhibitory window to only what is
464 necessary for blocking receptor responses.

465 Mormyrids have additional electrosensory systems, ampullary and mormyromast, used
466 for passive and active electrolocation, respectively. Corollary discharge plays a significant, but
467 different, role in these systems (von der Emde and Bell, 2003; Warren and Sawtell, 2016). The
468 primary afferents of ampullary receptors are spontaneously active and exhibit long lasting
469 spiking responses that generally peak more than 20 ms after the EOD (Bell and Russell, 1978).
470 The primary afferents of mormyromasts have less spontaneous activity, but exhibit long lasting
471 responses consisting of 2–8 spikes ~2 ms after the EOD (Bell, 1990b). Corollary discharge in
472 both systems works to subtract predictive sensory consequences of reafference by activating a
473 modifiable efference copy (i.e. ‘negative image’) through cerebellar-like circuitry in the ELL
474 cortex (Warren and Sawtell, 2016). In this circuit, the negative image is generated in synapses

475 between granule cells forming parallel fibers and principal cells through spike-timing-dependent
476 plasticity (Bell et al., 1997). While the granule cells receive stereotyped corollary discharge
477 inputs with short delays after the EOD command, their outputs are more temporally diverse and
478 delayed (Kennedy et al., 2014). This is an important feature to provide a temporal basis for
479 generating a sufficiently long negative image (~200 ms). Species with longer EOD durations
480 likely have longer-lasting responses, which would require even more temporal dispersion among
481 granule cells to generate a longer-lasting negative image. In addition, through a separate pathway,
482 corollary discharge input facilitates responses to afferent input from mormyromasts, thereby
483 selectively enhancing responses to reafferent EODs (Bell, 1990a). Here, too, species and
484 individual differences in EOD duration may require corollary discharge input with different time
485 courses.

486 What might be the source of species differences in the delay of corollary discharge
487 inhibition of the KO pathway? The command nucleus (CN) drives the EO to produce each EOD
488 through the medullary relay nucleus (MRN) and the EMN (Fig. 1A). The CN also provides
489 corollary discharge inhibition to the nELL through the bulbar command-associated nucleus
490 (BCA), the mesencephalic command-associated nucleus (MCA), and the sublemniscal nucleus
491 (slem) (Fig. 1A). Note that the EOD command waveform recorded from the EMN is almost
492 identical across species and independent of EOD duration (Fig. 6; Bennett, 1971; Bass and
493 Hopkins, 1983; Grant et al., 1986; Carlson, 2002b), suggesting that command circuitry does not
494 contribute to corollary discharge delays. Thus, the corollary discharge pathway must be adjusting
495 the corollary discharge delay (Fig. 1A; Bell et al., 1983). Since the BCA is involved in EOD
496 command circuitry (Fig. 1A), it is an unlikely locus for evolutionary change. In addition, if the
497 BCA contributes to the regulation of corollary discharge delay, this should influence all corollary

498 discharge pathways (Bell et al., 1983). In contrast to KO, ampullary afferents respond to both
499 outside-negative and outside-positive changes in voltage across the skin, and exhibit much
500 longer lasting responses (Bell and Russell, 1978). This indicates that the ampullary pathway
501 requires different corollary discharge timing from the KO pathway. The MCA is an interesting
502 candidate because it projects to precommand pathways that are involved in controlling the inter-
503 pulse interval (IPI) between EODs, and longer EODs require longer IPIs (von der Emde et al.,
504 2000; Carlson, 2002a, 2002b, 2003). In addition, the MCA indirectly provides corollary
505 discharge excitatory input to the cells that receive input from mormyromast primary afferents,
506 and this requires similarly precise timing as in the Knollenorgan pathway (Zipser and Bennett,
507 1976; Bell et al., 1995; Bell and von der Emde, 1995). Furthermore, corollary discharge-related
508 processing in the ampullary pathway is handled by a separate pathway that does not involve
509 MCA (Bell et al., 1983). Thus, a single delay mechanism operating in MCA could coordinate
510 appropriate delays to the Knollenorgan pathway, mormyomast pathway, and precommand
511 pathway, without affecting the ampullary pathway. It is also possible that a change in slem,
512 which receives excitatory input from MCA and directly inhibits nELL, could contribute to
513 regulating the corollary discharge delay we observed here. Future studies will compare this
514 corollary discharge pathway across species to identify the source of species differences in delay.

515 What might be the mechanism for species differences in the corollary discharge
516 inhibition delay? There are at least three types of modifications that could change this delay.
517 First, elongating axons could increase transmission delays much like the ‘delay lines’ observed
518 in several sensory systems (Carr and Konishi 1988; Lyons-Warren et al., 2013b). Second,
519 decreasing myelination and/or smaller axonal diameter could reduce the conduction velocity of
520 axonal action potential propagation (Waxman et al., 1972; Seidl, 2014). Third, intrinsic

521 properties of neurons (e.g. A-current, kinetics of transient outward K^+ current) can also affect
522 inhibition timing (Getting, 1983). A combination of physiological recording and anatomical
523 characterization of the corollary discharge pathway across species will uncover the mechanistic
524 basis for evolutionary change in corollary discharge inhibition delays.

525 In addition to species differences, we show that individual differences in corollary
526 discharge delay are correlated with delay to EOD peak 1 in *C. numenius* (Fig. 6). A previous
527 study demonstrated that EOD duration changes substantially with growth in *C. numenius*, and
528 this correlates with ontogenetic changes in EO anatomy (Paul et al., 2015). For many mormyrid
529 species, EOD waveform varies with ontogeny, sex, relative dominance, and season (Bass, 1986;
530 Hopkins, 1999; Carlson et al., 2000; Werneyer and Kramer, 2006). The existence of individual
531 variation in corollary discharge delays raises the question whether the same mechanism is used
532 for individual variation of corollary discharge as for species differences. Moreover, are changes
533 in corollary discharge timing and EOD duration mediated by a shared central regulatory pathway,
534 or through neuronal plasticity associated with changing sensory input in response to self-
535 generated EODs?

536 There are at least three possibilities that might explain how corollary discharge delay
537 changes along with individual or evolutionary change in EOD waveform: (1) EOD command
538 pathway drives both changes in EOD waveform and corollary discharge delay; (2) genetic
539 regulation drives both changes; (3) neural plasticity adapts the corollary discharge to changes in
540 EOD duration. (1) would be impossible because there is no way for the electromotor network to
541 provide the corollary discharge pathway with waveform information. EOD waveform is
542 determined by the biophysical characteristics of electrocytes (Bennett, 1971; Bass, 1986),
543 independent from the EOD command (Fig. 5; Bass and Hopkins, 1983). (2) would be possible.

544 Recently, the genomic basis of EO anatomy and physiology is being increasingly well studied
545 (Gallant et al., 2014; Gallant and O’Connell, 2020). It would be interesting if a central regulatory
546 mechanism lead to correlated transcriptional changes in the EO and corollary discharge pathway.
547 (3) would be possible. Although previous studies suggest that corollary discharge in the KO
548 system is invariant over several hours of electrophysiological experimentation, this was under a
549 limited, unnatural situation in which the EOD was absent and no association with an alternative
550 EOD was tested (Bell and Grant, 1989). Such an associative mechanism possibly takes place in
551 the nELL as it is only site at which corollary discharge and KO sensory processing converge
552 (Mugnaini and Maler, 1987). However, it is possible that retrograde signals could make an
553 association at earlier stages in the corollary discharge pathway.

554 The inter-species variance of corollary discharge delays had a 1:1 correspondence with
555 delays to EOD peak 1, because the slopes of the regression lines were nearly 1 (Fig. 4D, E). By
556 contrast, for intra-species variance in *C. numenius*, these slopes were less than 0.5 (Fig. 7),
557 indicating that fish with longer EODs have earlier corollary discharge delays than would be
558 expected from the delay to EOD peak 1. The reason remains unclear, but one possibility is that a
559 plasticity-based mechanism governs a shift in the corollary discharge delay, and there may be a
560 ‘lag time’ in the response of the corollary discharge circuit to EOD elongation during
561 development.

562 Here we show evolutionary change of corollary discharge inhibition for the first time.
563 Our results strongly suggest a corollary discharge pathway makes an appropriate delay to block
564 receptor responses to self-generated signals. Future studies will seek to identify the source of
565 delays and the cellular mechanisms using electrophysiological and anatomical approaches.
566 Furthermore, it will be interesting to study time shifts of corollary discharge inhibition during

- 567 signal development within individuals. Such studies will reveal the mechanisms by which
- 568 sensorimotor integration is adjusted to account for species and individual differences in behavior.

569 **REFERENCES**

- 570 Amagai S (1998) Time coding in the midbrain of mormyrid electric fish. II. Stimulus selectivity
571 in the nucleus exterolateralis pars posterior. *J Comp Physiol A* 182:131–143.
- 572 Arnegard ME, McIntyre PB, Harmon LJ, Zelditch ML, Crampton WG, Davis JK, Sullivan JP,
573 Lavoué S, Hopkins CD (2010) Sexual signal evolution outpaces ecological divergence
574 during electric fish species radiation. *Am Nat* 176:335–356.
- 575 Baker CA, Kohashi T, Lyons-Warren AM, Ma X, Carlson BA (2013) Multiplexed temporal
576 coding of electric communication signals in mormyrid fishes. *J Exp Biol* 216:2365–2379.
- 577 Baker CA, Huck KR, Carlson BA (2015) Peripheral sensory coding through oscillatory
578 synchrony in weakly electric fish. *eLife* 4:e08163.
- 579 Bass AH (1986) Species differences in electric organs of mormyrids: Substrates for species-
580 typical electric organ discharge waveforms. *J Comp Neurol* 244:313–330.
- 581 Bass AH, Hopkins CD (1983) Hormonal control of sexual differentiation: change of electric
582 organ discharge waveform. *Science* 220:971–974.
- 583 Bass AH, Hopkins CD (1984) Shifts in frequency tuning of electroreceptors in androgen-treated
584 mormyrid fish. *J Comp Physiol A* 155:713–724.
- 585 Bell CC (1989) Sensory coding and corollary discharge effects in mormyrid electric fish. *J Exp*
586 *Biol* 146:229–253.
- 587 Bell CC (1990a) Mormyromast electroreceptor organs and their afferent fibers in mormyrid fish.
588 II. Intra-axonal recordings show initial stages of central processing. *J Neurophysiol* 63:303–
589 318.

- 590 Bell CC (1990b) Mormyromast electroreceptor organs and their afferent fibers in mormyrid fish.
591 III. Physiological differences between two morphological types of fibers. *J Neurophysiol*
592 63:319–332.
- 593 Bell CC, Russell CJ (1978) Effect of electric organ discharge on ampullary receptors in a
594 mormyrid. *Brain Res* 145:85–96.
- 595 Bell C, Grant K (1989) Corollary discharge inhibition and preservation of temporal information
596 in a sensory nucleus of mormyrid electric fish. *J Neurosci* 9:1029–1044.
- 597 Bell C, von der Emde G (1995) Electric organ corollary discharge pathways in mormyrid fish. II.
598 The medial juxtalobar nucleus. *J Comp Physiol A* 177:463–479.
- 599 Bell C, Libouban S, Szabo T (1983) Pathways of the electric organ discharge command and its
600 corollary discharges in mormyrid fish. *J Comp Neurol* 216:327–338.
- 601 Bell C, Dunn K, Hall C, Caputi A (1995) Electric organ corollary discharge pathways in
602 mormyrid fish. I. The mesencephalic command associated nucleus. *J Comp Physiol A*
603 177:449–462.
- 604 Bell CC, Han VZ, Sugawara Y, Grant K (1997) Synaptic plasticity in a cerebellum-like structure
605 depends on temporal order. *Nature* 387:279–281.
- 606 Bennett MVL (1965) Electroreceptors in Mormyrids. *Cold Spring Harb Sym* 30:245–262.
- 607 Bennett MVL (1971) Electric organs. *Fish Physiol* 5:347–491.
- 608 Carlson BA (2002a) Electric signaling behavior and the mechanisms of electric organ discharge
609 production in mormyrid fish. *J Physiol (Paris)* 96:405–419.
- 610 Carlson BA (2002b) Neuroanatomy of the mormyrid electromotor control system. *J Comp*
611 *Neurol* 454:440–455.

- 612 Carlson BA (2003) Single-unit activity patterns in nuclei that control the electromotor command
613 nucleus during spontaneous electric signal production in the mormyrid *Brienomyrus*
614 *brachyistius*. *J Neurosci* 23:10128–10136.
- 615 Carlson BA (2009) Temporal-pattern recognition by single neurons in a sensory pathway
616 devoted to social communication behavior. *J Neurosci* 29:9417–9428.
- 617 Carlson BA, Hopkins CD, Thomas P (2000) Androgen correlates of socially induced changes in
618 the electric organ discharge waveform of a mormyrid fish. *Horm Behav* 38:177–186.
- 619 Carlson BA, Hasan SM, Hollmann M, Miller DB, Harmon LJ, Arnegard ME (2011) Brain
620 evolution triggers increased diversification of electric fishes. *Science* 332:583–586.
- 621 Carr CE, Konishi M (1988) Axonal delay lines for time measurement in the owl's brainstem.
622 *Proc Natl Acad Sci USA* 85:8311–8315.
- 623 Crapse TB, Sommer MA (2008) Corollary discharge across the animal kingdom. *Nat Rev*
624 *Neurosci* 9:587–600.
- 625 Ding Y, Lillvis JL, Cande J, Berman GJ, Arthur BJ, Long X, Xu M, Dickson BJ, Stern DL
626 (2019) Neural evolution of context-dependent fly song. *Curr Biol* 29:1089–1099.
- 627 Einevoll GT, Kayser C, Logothetis NK, Panzeri S (2013) Modelling and analysis of local field
628 potentials for studying the function of cortical circuits. *Nat Rev Neurosci* 14:770–785.
- 629 von der Emde G (1999) Active electrolocation of objects in weakly electric fish. *J Exp Biol*
630 202:1205–1215.
- 631 von der Emde G, Bell CC (2003) Active electrolocation and its neural processing in mormyrid
632 electric fishes. In: *Sensory Processing in Aquatic Environments* (Collin SP and Marshall J,
633 ed), pp92–107. New York: Springer.

- 634 von der Emde G, Sena LG, Niso R, Grant K (2000) The midbrain precommand nucleus of the
635 mormyrid electromotor network. *J Neurosci* 20:5482–5495.
- 636 Feulner PGD, Kirschbaum F, Tiedemann R (2008) Adaptive radiation in the Congo River: An
637 ecological speciation scenario for African weakly electric fish (Teleostei; Mormyridae;
638 *Campylomormyrus*). *J Physiol (Paris)* 102:340–346.
- 639 Gallant JR, O’Connell LA (2020) Studying convergent evolution to relate genotype to behavioral
640 phenotype. *J Exp Biol* 223 (Suppl 1):jeb213447.
- 641 Gallant JR, Traeger LL, Volkening JD, Moffett H, Chen P-H, Novina CD, Phillips GN, Anand R,
642 Wells GB, Pinch M, Güth R, Unguez GA, Albert JS, Zakon HH, Samanta MP, Sussman
643 MR (2014) Genomic basis for the convergent evolution of electric organs. *Science*
644 344:1522–1525.
- 645 Getting PA (1983) Mechanisms of pattern generation underlying swimming in *Tritonia*. III.
646 Intrinsic and synaptic mechanisms for delayed excitation. *J Neurophysiol* 49:1036–1050.
- 647 Grafen A (1989) The phylogenetic regression. *Phil Trans R Soc B* 326:119–157.
- 648 Grant K, Bell CC, Clause S, Ravaille M (1986) Morphology and physiology of the brainstem
649 nuclei controlling the electric organ discharge in mormyrid fish. *J Comp Neurol* 245:514–
650 530.
- 651 ter Hofstede HM, Schöneich S, Robillard T, Hedwig B (2015) Evolution of a communication
652 system by sensory exploitation of startle behavior. *Curr Biol* 25:3245–3252.
- 653 von Holst E, Mittelstaedt H (1950) Das reafferenzprinzip. *Naturwissenschaften* 37:464–476
- 654 Hopkins CD (1981) On the diversity of electric signals in a community of mormyrid electric fish
655 in west Africa. *Am Zool* 21:211–222.
- 656 Hopkins CD (1999) Design features for electric communication. *J Exp Biol* 202:1217–1228.

- 657 Hopkins CD, Bass AH (1981) Temporal coding of species recognition signals in an electric fish.
658 Science 212:85–87.
- 659 Jacob PF, Hedwig B (2019) Structure, Activity and function of a singing CPG interneuron
660 controlling cricket species-specific acoustic signaling. J Neurosci 39:96–111.
- 661 Katz PS (2011) Neural mechanisms underlying the evolvability of behaviour. Phil Trans R Soc B
662 366:2086–2099.
- 663 Katz PS (2016) Evolution of central pattern generators and rhythmic behaviours. Phil Trans R
664 Soc B 371:20150057.
- 665 Kennedy A, Wayne G, Kaifosh P, Alviña K, Abbott L, Sawtell NB (2014) A temporal basis for
666 predicting the sensory consequences of motor commands in an electric fish. Nat Neurosci
667 17:416–422.
- 668 Kwong-Brown U, Tobias ML, Elias DO, Hall IC, Elemans CP, Kelley DB (2019) The return to
669 water in ancestral *Xenopus* was accompanied by a novel mechanism for producing and
670 shaping vocal signals. eLife 8:e39946.
- 671 Lavoué S, Sullivan JP, Hopkins CD (2003) Phylogenetic utility of the first two introns of the *S7*
672 ribosomal protein gene in African electric fishes (Mormyroidea: Teleostei) and congruence
673 with other molecular markers. Biol J Linn Soc 78:273–292.
- 674 Lyons-Warren AM, Hollmann M, Carlson BA (2012) Sensory receptor diversity establishes a
675 peripheral population code for stimulus duration at low intensities. J Exp Biol 215:2586–
676 2600.
- 677 Lyons-Warren AM, Kohashi T, Mennerick S, Carlson BA (2013a) Retrograde fluorescent
678 labeling allows for targeted extracellular single-unit recording from identified neurons in
679 vivo. J Vis Exp 76:e3921.

- 680 Lyons-Warren AM, Kohashi T, Mennerick S, Carlson BA (2013b) Detection of submillisecond
681 spike timing differences based on delay-line anticoincidence detection. *J Neurophysiol*
682 110:2295–2311.
- 683 Martin GR (2012) Through birds' eyes: insights into avian sensory ecology. *J Ornithol* 153:23–
684 48.
- 685 Mugnaini E, Maler L (1987) Cytology and immunocytochemistry of the nucleus of the lateral
686 line lobe in the electric fish *Gnathonemus petersii* (mormyridae): Evidence suggesting that
687 GABAergic synapses mediate an inhibitory corollary discharge. *Synapse* 1:32–56.
- 688 Mundry R (2014) Statistical issues and assumptions of phylogenetic generalized least squares.
689 In: *Modern Phylogenetic Comparative Methods and Their Application in Evolutionary*
690 *Biology, Concepts and Practice* (Garamszegi LZ ed), pp131–153. Berlin Heidelberg:
691 Springer.
- 692 Osorio D, Vorobyev M (2008) A review of the evolution of animal colour vision and visual
693 communication signals. *Vision Res* 48:2042–2051.
- 694 Otte, D (1992) Evolution of cricket songs. *J Orthop Res* 1:25–49.
- 695 Paradis E. & Schliep K (2018) ape 5.0: an environment for modern phylogenetics and
696 evolutionary analyses in R. *Bioinformatics* 35:526–528.
- 697 Paul C, Mamonekene V, Vater M, Feulner PGD, Engelmann J, Tiedemann R, Kirschbaum F
698 (2015) Comparative histology of the adult electric organ among four species of the genus
699 *Campylomormyrus* (Teleostei: Mormyridae). *J Comp Physiol A* 201:357–374.
- 700 Pinheiro J, Bates D, DebRoy S, Sarkar D, R Core Team (2020) nlme: linear and nonlinear mixed
701 effects models. R package version 3.1-145. <https://CRAN.R-project.org/package=nlme>.

- 702 Podos J (2001) Correlated evolution of morphology and vocal signal structure in Darwin's
703 finches. *Nature* 409:185–188.
- 704 Poulet JF, Hedwig B (2006) The cellular basis of a corollary discharge. *Science* 311:518–522
- 705 Poulet JF, Hedwig B (2007) New insights into corollary discharges mediated by identified neural
706 pathways. *Trend Neurosci* 30:14–21.
- 707 Russell CJ, Bell CC (1978) Neuronal responses to electrosensory input in mormyrid valvula
708 cerebelli. *J Neurophysiol* 41:1495–1510.
- 709 Schneider DM, Mooney R (2018) How movement modulates hearing. *Annu Rev Neurosci*
710 41:553–572.
- 711 Seeholzer LF, Seppo M, Stern DL, Ruta V (2018) Evolution of a central neural circuit underlies
712 *Drosophila* mate preferences. *Nature* 559:564–569.
- 713 Seidl AH (2014) Regulation of conduction time along axons. *Neuroscience* 276:126–134.
- 714 Silva L, Antunes A (2016) Vomeronasal receptors in vertebrates and the evolution of pheromone
715 detection. *Annu Rev Anim Biosci* 5:353–370.
- 716 Sperry RW (1950) Neural basis of the spontaneous optokinetic response produced by visual
717 inversion. *J Comp Physiol Psych* 43:482–489.
- 718 Stöckl AL, Kelber A (2019) Fuelling on the wing: sensory ecology of hawkmoth foraging. *J*
719 *Comp Physiol A* 205:399–413.
- 720 Straka H, Simmers J, Chagnaud BP (2018) A new perspective on predictive motor signaling.
721 *Curr Biol* 28:R232–R243.
- 722 Sukhum KV, Shen J, Carlson BA (2018) Extreme enlargement of the cerebellum in a clade of
723 teleost fishes that evolved a novel active sensory system. *Curr Biol* 28:3857–3863.

- 724 Sullivan JP, Lavoué S, Hopkins CD (2000) Molecular systematics of the African electric fishes
725 (Mormyroidea: teleostei) and a model for the evolution of their electric organs. *J Exp Biol*
726 203:665–683.
- 727 Trzcinski N (2008) Electric signaling and Knollenorgan receptor organ properties in the genus
728 *Campylomormyrus* (Mormyridae). Neurobiology and Behavior Honors Thesis, Cornell
729 University.
- 730 Trzcinski N, Hopkins CD (2008) Electric signaling and electroreception properties in electric
731 fishes of the genus *Campylomormyrus* (Mormyridae). *Cornell Synapse* 2:19–22.
- 732 Vélez A, Carlson BA (2016) Detection of transient synchrony across oscillating receptors by the
733 central electrosensory system of mormyrid fish. *eLife* 5:e16851.
- 734 Vélez A, Kohashi T, Lu A, Carlson BA (2017) The cellular and circuit basis for evolutionary
735 change in sensory perception in mormyrid fishes. *Sci Rep* 7:3783.
- 736 Warren R, Sawtell NB (2016) A comparative approach to cerebellar function: insights from
737 electrosensory systems. *Curr Opin Neurobiol* 41:31–37.
- 738 Waxman SG, Pappas GD, Bennett MVL (1972) Morphological correlates of functional
739 differentiation of nodes of Ranvier along single along single fibers in the neurogenetic
740 electric organ of the knife fish *Sternarchus*. *J Cell Biol* 53:210–224.
- 741 Werneyer M, Kramer B (2006) Ontogenetic development of electric-organ discharges in a
742 mormyrid fish, the bulldog *Marcusenius macrolepidotus* (South African form). *J Fish Biol*
743 69:1190–1201.
- 744 Xu-Friedman M, Hopkins C (1999) Central mechanisms of temporal analysis in the
745 knollenorgan pathway of mormyrid electric fish. *J Exp Biol* 202:1311–1318.

746 Zipser B, Bennett MVL (1976) Interaction of electrosensory and electromotor signals in lateral
747 line lobe of a mormyrid fish. *J Neurophysiol* 39:713–721.
748

749 **FIGURE LEGENDS**750 **Figure 1. Corollary discharge inhibition and evolution of EOD duration. (A)**

751 Diagram showing electromotor (blue), Knollenorgan sensory (red), and corollary discharge
752 (purple) pathways. The command nucleus (CN) drives the EO to generate each EOD via the
753 medullary relay nucleus (MRN) and the spinal electromotor neurons (EMN). Knollenorgan
754 electroreceptors (KO) receive the EOD and send time-locked spikes to the nucleus of the
755 electrosensory lateral line lobe (nELL) via primary afferents. The nELL neurons project their
756 axons to the anterior extrolateral nucleus (ELa), which sends its only output to the adjacent
757 posterior EL (ELp). The CN provides another output to the bulbar command-associated nucleus
758 (BCA), which in turn projects to the MRN and to the mesencephalic command-associated
759 nucleus (MCA). The MCA sends its output to the sublemniscal nucleus (slem) that has
760 GABAergic neurons projecting to the nELL. ELL, electrosensory lateral lobe; OB, olfactory
761 bulb; OT, optic tectum; tel, telencephalon; val, valvula of the cerebellum. (B) Potential
762 hypothesis of corollary discharge inhibition between mormyrids with short EOD and long EOD.
763 The schematic diagram shows spike timings of the CN and EMN as well as EOD. The purple
764 rectangle indicates the potential time window of corollary discharge inhibition (CDI). In the
765 short-EOD species, the corollary discharge covers the KO spike to self-generated EODs so as to
766 inhibit sensory responses in the nELL. Since long-duration EODs can cause KO spikes with
767 different timing, corollary discharge inhibition needs to change its duration and/or timing to
768 block reafferent responses in the nELL.

769

770 **Figure 2. Mormyrids generate species-specific electric organ discharges (EODs). (A)**

771 Cladogram based on consensus trees of the species studied (Sullivan et al., 2000; Lavoué et al.,

772 2003; Feulner et al., 2008; Sukhum et al., 2018). EOD traces are plotted as overlays of
773 waveforms recorded from N individuals of each species and aligned to peak 1, defined as the
774 head-positive peak. The EODs in *C. numenius* are displayed in three categories with distinct
775 EOD durations (Long, Intermediate and Short). Expanded EODs for all other species are shown
776 in the dotted box to the right. (B) Box plots of EOD durations from each species, sorted by EOD
777 duration. (C) Power spectra of EODs from each species, from the same individuals shown in A.
778 Each trace indicates the average EOD power spectrum from one individual. (D) Summary of
779 EOD power spectra. Each bold line inside the box indicates the mean peak power frequency. The
780 box limits indicate the mean lower and higher frequencies 3 dB below the peak. Error bars
781 indicate the standard error of the mean.

782

783 **Figure 3. Corollary discharge inhibition in the communication circuit varies in**
784 **timing and duration among mormyrid species.** (A) Schematic representation of
785 electrophysiological recording from the fish. An extracellular electrode inside a tube placed over
786 the tail records EOD commands from spinal electromotor neurons (EMN). To assess corollary
787 discharge inhibition related to EOD production, we delivered sensory stimuli at different delays
788 (0–20 ms) after the EOD command (EODC) onset, which is determined as the first negative peak
789 (indicated by black arrowhead), while recording evoked potentials in ELa or ELp. (B)
790 Representative mean evoked potentials (n = 10 traces) obtained from ELa and ELp in *M. tapirus*.
791 (D) Representative mean evoked potentials in response to stimuli at varying delays following the
792 EOD command (0–8 ms) in *C. compressirostris* and *C. numenius* (Long EOD type). (E)
793 Summary of corollary discharge inhibition across species. Inset describes the measurement of
794 corollary discharge inhibition timing. The response magnitudes of evoked potentials were

795 calculated as the peak-to-peak amplitude (blue bars) and normalized to the maximum peak-to-
796 peak amplitude across all stimulus delays. Using an 80% threshold, we determined inhibition
797 onset, offset, and duration (red bar). The large point on the red bar indicates the peak inhibition
798 time. Left and right panels show the inhibition periods relative to the EOD command in ELa and
799 ELp, respectively, across all individuals studied.

800

801 **Figure 4. Corollary discharge inhibition onset is correlated with EOD duration.** (A,
802 B) Plots of inhibition duration (y axis) against EOD duration (x axis) in ELa and ELp. (C, D)
803 Plots of inhibition onset against EOD duration in ELa and ELp. (E, F) Plots of inhibition onset
804 against delay to peak 1 of the EOD in ELa and ELp. Points show the mean value of species \pm the
805 standard deviation (but not for *C. numenius*). Regression lines were determined using a PGLS
806 analysis. Significant correlations are indicated by a solid line and insignificant correlations are
807 indicated by a dotted line. Although *C. numenius* is represented as three groups (long,
808 intermediate and short EOD), the regression was calculated using average values of each species.
809 The estimated slope, 95% confidence interval (CI) and the p-value are shown in each plot.

810

811 **Figure 5. Knollenorgans respond with time-locked spikes following peak 1 of EOD**
812 **stimuli that simulate self-generated EODs.** (A) Example traces of normalized KO responses of
813 *C. compressirostris*, *B. brachyistius*, and *C. numenius*. Lower traces show the inverted EODs of
814 conspecifics whose onsets are aligned to time 0. (B) Plots of delay to peak KO response against
815 delay to peak 1 of EOD. Points show the mean value of species \pm the standard deviation.
816 Regression line was determined using a PGLS analysis. The estimated slope, 95% confidence
817 interval (CI) and the p-value are shown.

818

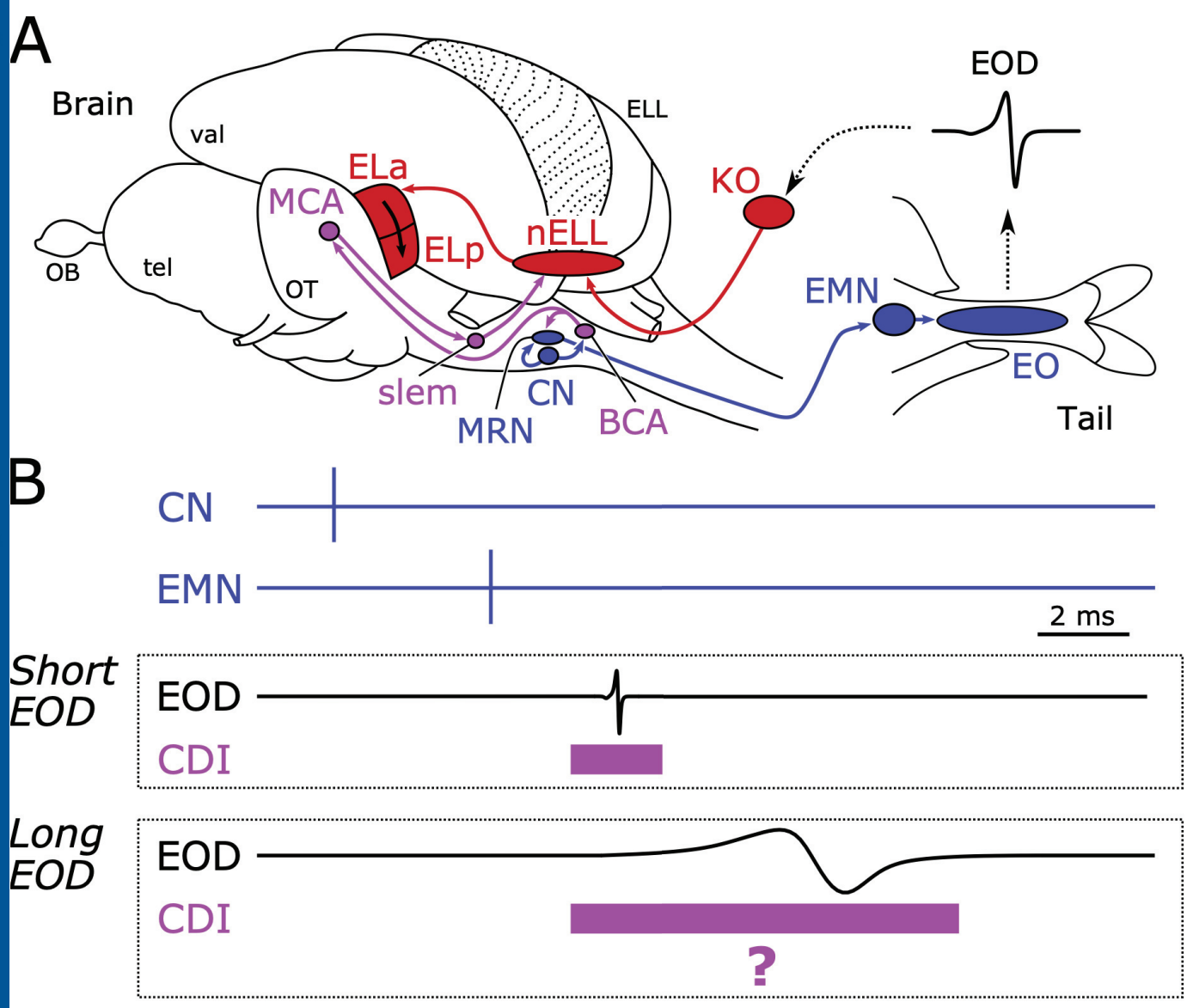
819 **Figure 6. Corollary discharge inhibition is timed to block responses to peak 1 of the**
820 **EOD.** We compared the time courses of the EOD command (EODC) (upper blue traces), the
821 EOD (middle traces), and corollary discharge inhibition. Vertical dotted lines indicate EODC
822 onset (black), EOD onset (green), and peak 1 of the EOD (red). D_{onset} , Delay to EOD onset; D_{P1} ,
823 Delay to peak 1 of EOD.

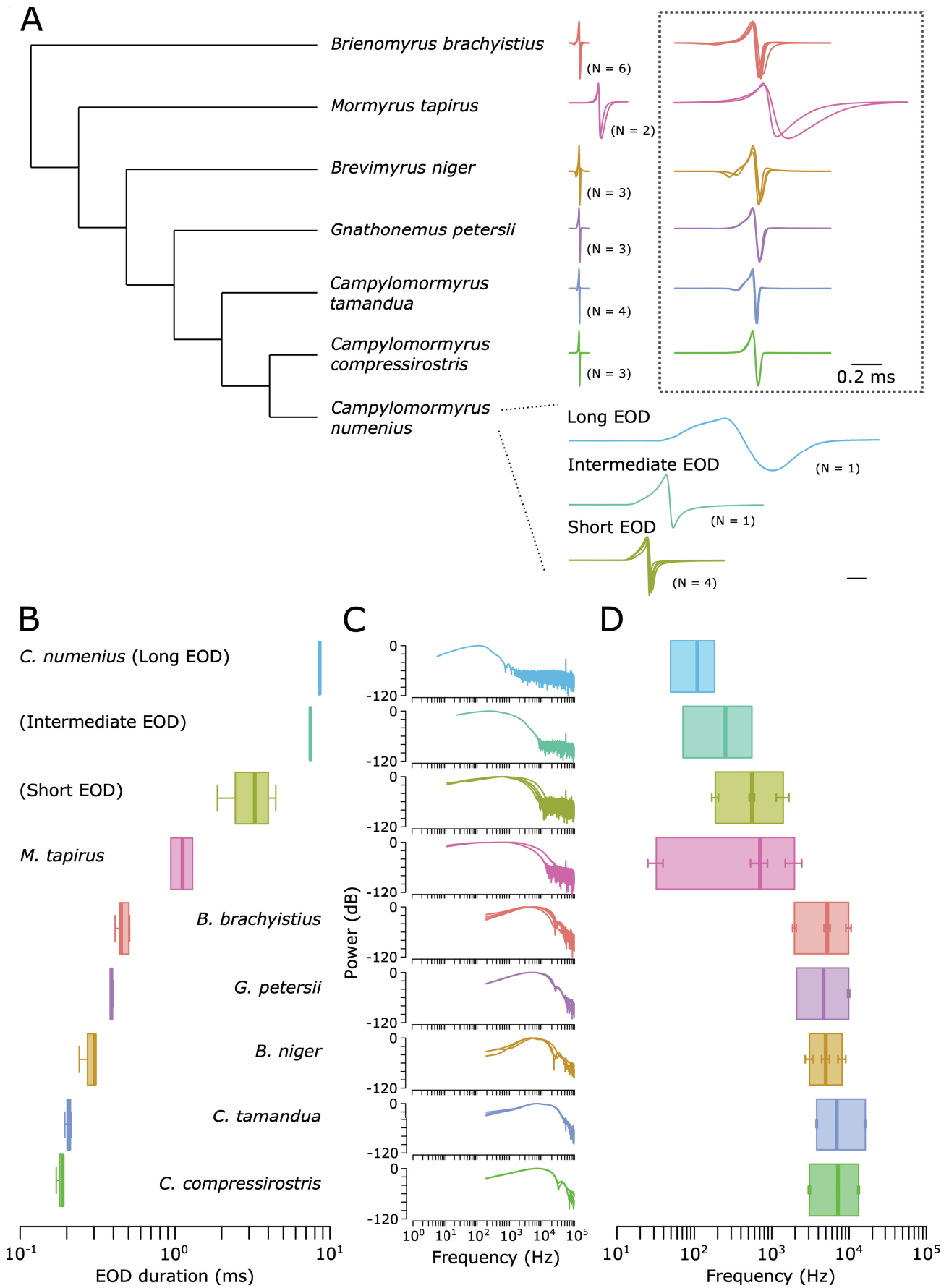
824

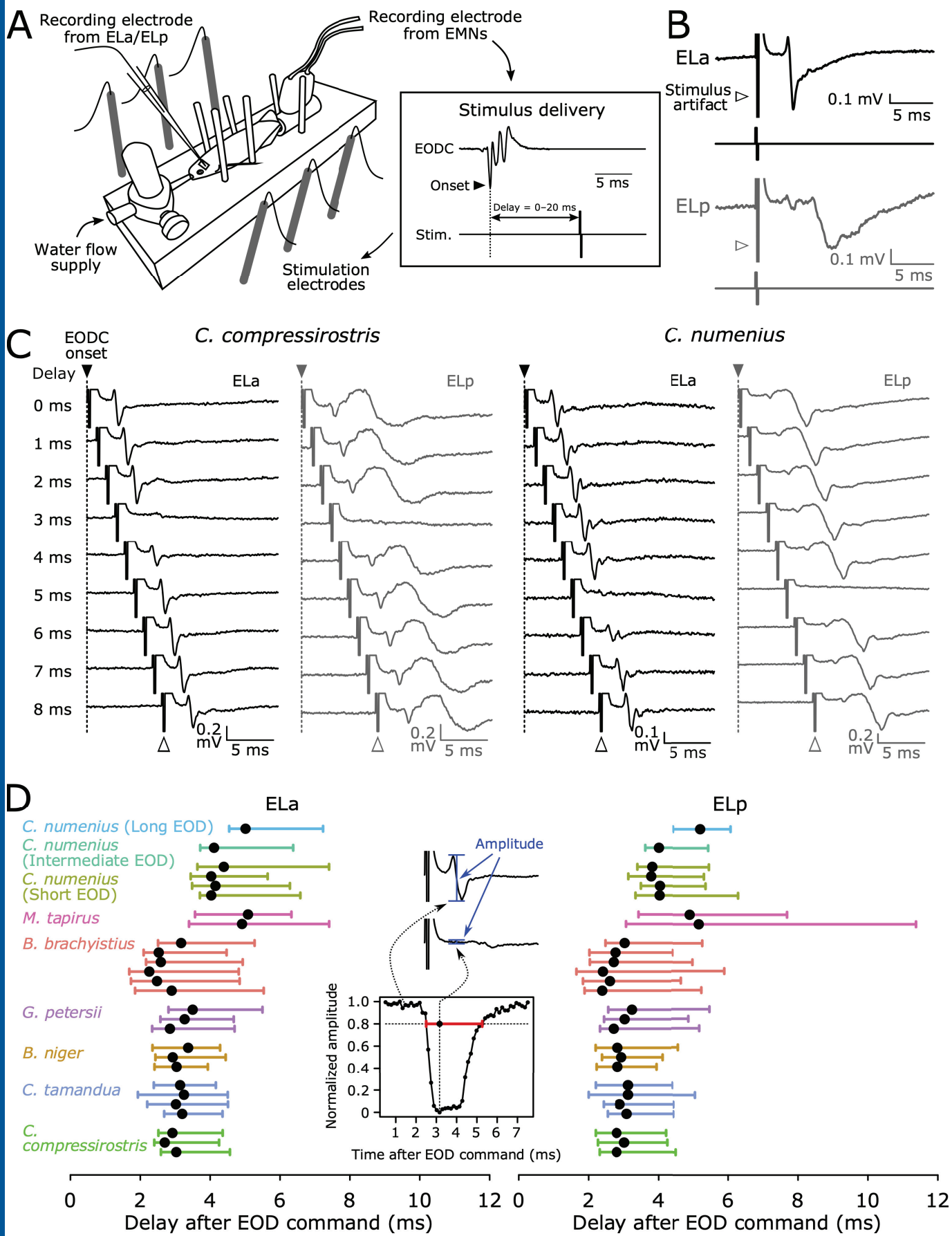
825 **Figure 7. Corollary discharge onset is correlated with individual EOD waveform**
826 **variation among *C. numenius*.** Plots of inhibition onset (y axis) against delay to peak 1 of EOD
827 (x axis) in ELa and ELp. Points show individual values. Regression lines were determined using
828 a linear regression analysis. R , Pearson's correlation coefficient; P , p -value of the correlation.
829 The estimated slope, 95% confidence interval (CI) and the p -value are shown.

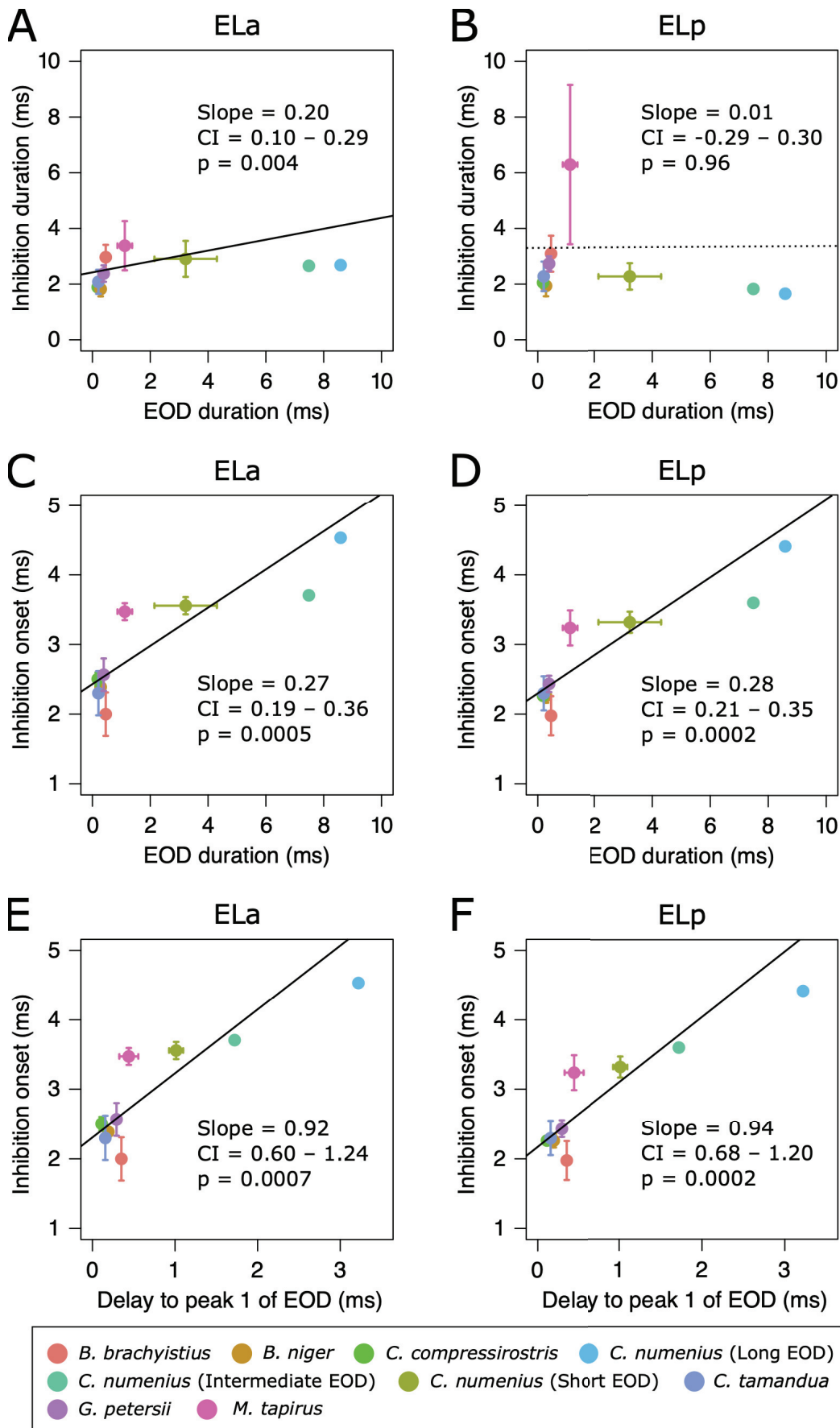
830

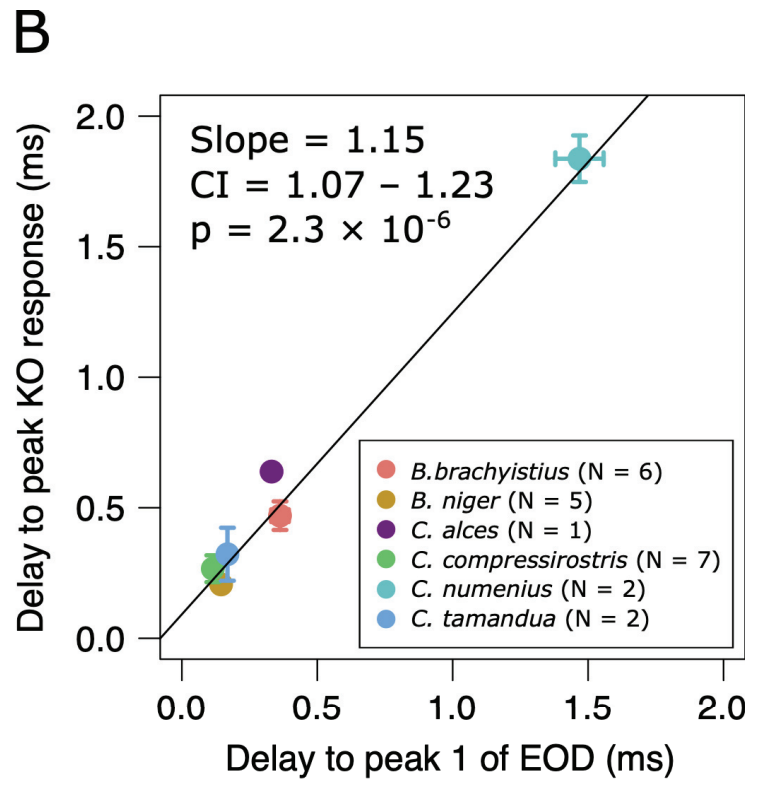
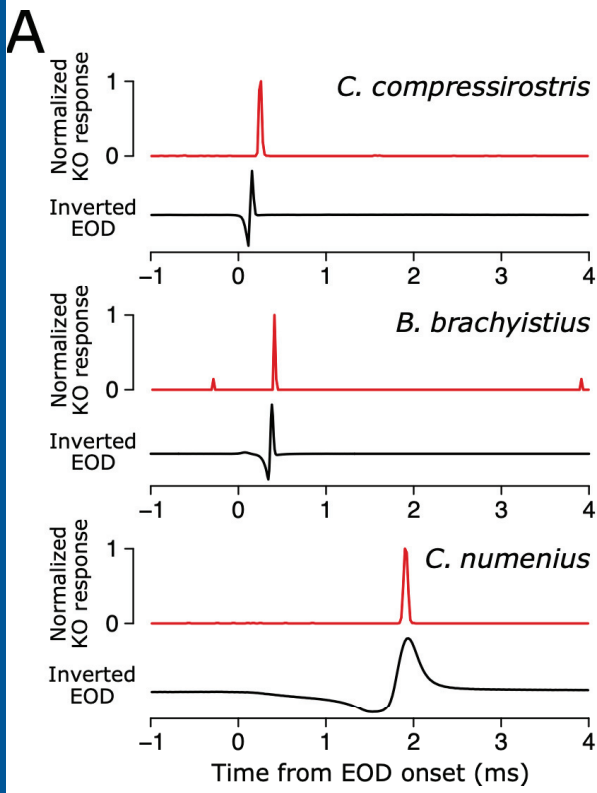
831 **Figure 8. Time shift of corollary discharge inhibition underlies communication**
832 **signal evolution in mormyrid.** (A) Summary of corollary discharges between mormyrids with
833 short-duration EOD and long-duration EOD. The schematic diagram shows spike timings of
834 EMN and KO as well as EOD. Purple rectangle shows time window of corollary discharge
835 inhibition (CDI).

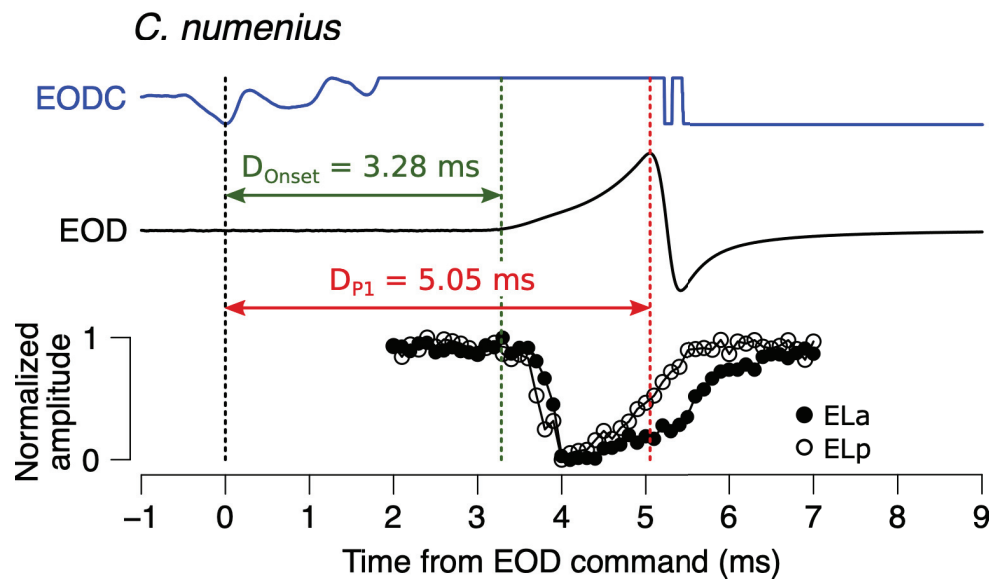
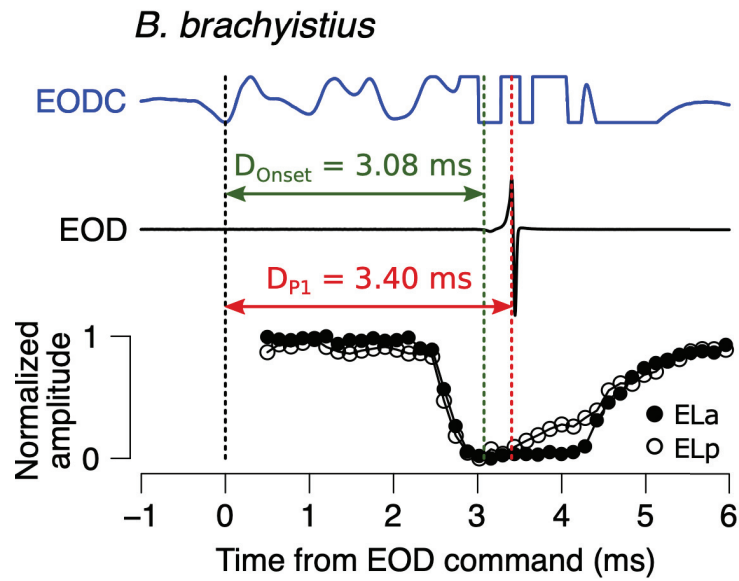
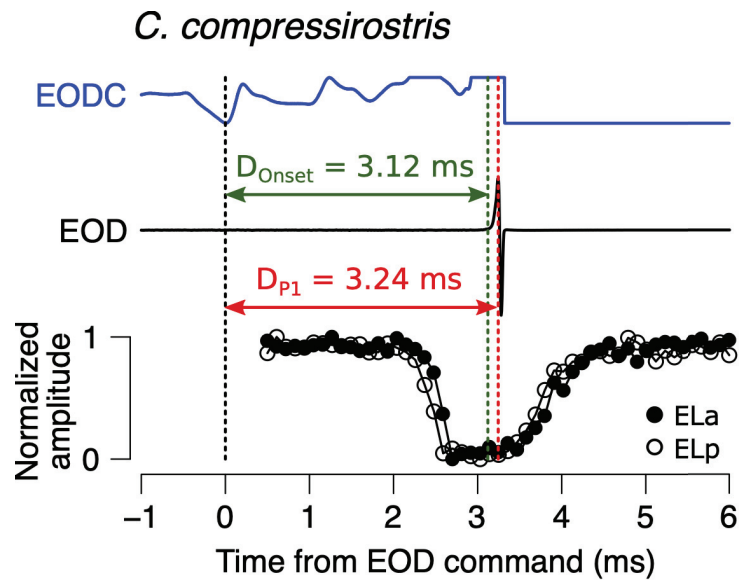


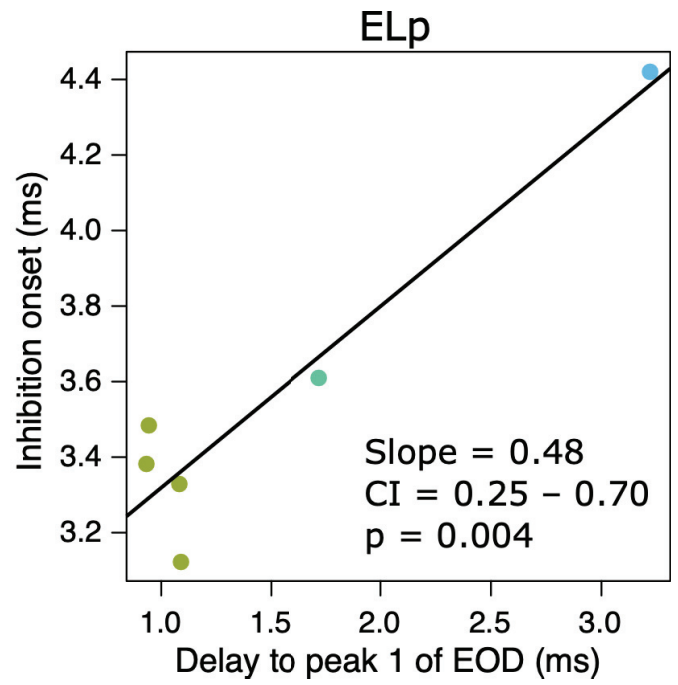
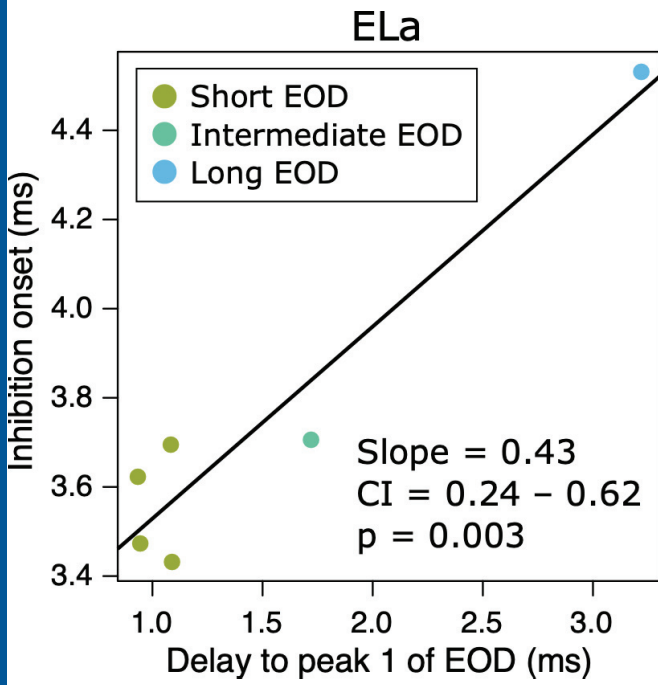






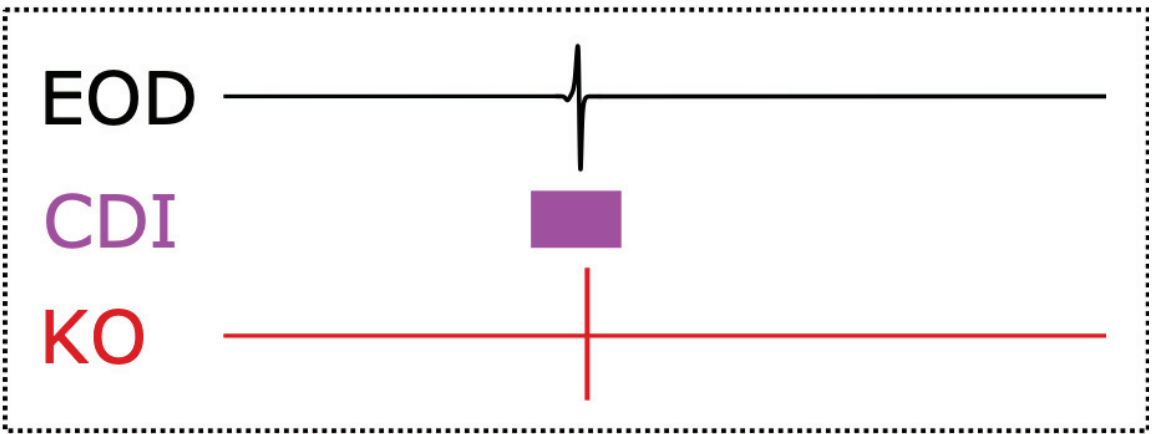








Short EOD



Long EOD

